Modelling lake water and isotope mass balance variations under Mediterranean climate: Lake Azigza in the Moroccan Middle Atlas

Rachid Adallal, Christine Vallet-Coulomb, Laurence Vidal, Abdelfattah Benkaddour, Ali Rhoujjati, Corinne Sonzogni

Modelling lake water and isotope mass balance variations under Mediterranean climate: Lake Azigza in the Moroccan Middle Atlas

Rachid Adallal[1,2*], Christine Vallet-Coulomb[1] (vallet@cerege.fr), Laurence Vidal[1] (vidal@cerege.fr), Abdelfattah Benkaddour[2] (a.benkaddour@uca.ma), Ali Rhoujjati[2] (a.rhoujjati@uca.ma), Corinne Sonzogni[1] (sonzogni@cerege.fr)

[1]Aix Marseille Univ, CNRS, IRD, INRA, Coll France, CEREGE, Aix en Provence, France
[2]Laboratoire de Géo-ressources, Unité associée au CNRST (URAC 42), Faculté des Sciences et Techniques, Université Cadi Ayyad, Marrakech, Morocco

Short title: Modelling lake variations in the Moroccan Middle Atlas

**Corresponding author*: Rachid Adallal (adallal@cerege.fr; adallal.r@gmail.com)

Adresse 1 : CEREGE, BP80, 13545, Aix-en-Provence, cedex 4, France, tel : +33751310087

Adresse 2 : Université Cadi Ayyad, Laboratoire de Géo-ressources, BP549, Av. Abdelkarim El Khattabi, Marrakech, Morocco, tel : +212677848801

Abstract

As many Mediterranean headwater catchments, the Moroccan Middle Atlas plays an important role in the highly vulnerable regional water resources. Mountain lakes are numerous in this region, and could be regarded as possible sentinels of hydro-climatic changes, using appropriate modelling tools able to simulate the lake-climate relation. We present a detailed study of Lake Azigza, based on a 4-year (2012-2016) observation period, including lake level measurements, isotope analyses of precipitation, lake and spring waters, and local meteorological data. The approach is based on a step-by-step calibration of a lake water balance model, fed by precipitation and evaporation rates, to estimate the ungauged components of the water balance. The net groundwater balance (inflow *minus* outflow) was quantified during periods deprived of precipitation and further interpolated for the whole period. Diffuse surface runoff was estimated through the adjustment of a rainfall coefficient. Finally, the groundwater fluxes were partitioned between inflow and outflow using the isotope mass balance. The model was able to simulate the continuous lake level decrease (4 m) observed over 2012-2016. Results show the dominance of groundwater exchanges in the lake water balance, with significant interannual variations related to annual precipitation, suggesting that a threshold effect probably limits the seepage when the lake level decreases. This study underlines the importance of groundwater fluxes in the lake level variations for Lake Azigza, probably representative of many similar lakes in the Middle Atlas.

Keywords

Lake level, stable isotopes, lake-groundwater exchanges, Middle Atlas

Length of the manuscript: 8759 word

Introduction

The Mediterranean region is considered by the latest IPCC report to be a ‘‘Hot-Spot’’ for global climate change (IPCC 2013). In the last decades, temperature rise was above the global average and model projections indicate a warming and drying trend in the Mediterranean basin (Lionello et al. 2014). In the southern part of the Mediterranean, Morocco constitutes a key area for assessing the impact and sensitivity of the water cycle to global climate change. Moroccan climate is influenced by air masses with various origin (Atlantic Ocean, Mediterranean Sea and Sahara), in addition to the effect of orography in the Atlas region, which leads to a marked spatial and inter-annual variability in precipitation. Several studies have already emphasized that precipitation records of the last decades showed a decrease in precipitation totals and wet days in Morocco (Driouech et al. 2010; Tramblay et al. 2013a) although heterogeneous behavior can be found at local scale (Khomsi et al. 2016). Future projections based on high resolution regional climate models (RCM) have forecasted a decrease in average precipitation following a north to south gradient for the end of the century (Tramblay et al. 2013b; Filahi et al. 2017).

Quantifying the impact of these future precipitation changes on water resources requires long-term hydrological data to validate model scenarios. An amplified response of runoff to precipitation decrease is expected (Tramblay et al. 2013b), but further studies are needed to explore the link between water cycle and climate variations. Lakes have often been regarded as representative indicators of the effect of climate variations on the water cycle at different times scales (Legesse et al. 2004; Vallet-Coulomb et al. 2006; Troin et al. 2010; Lyons et al. 2011; Haghighi and Klove 2015; Troin et al. 2016), providing an appropriate quantification of lake-groundwater exchanges, which have a great impact on lake behavior (Rosenberry et al. 2015; Jones et al. 2016). Stable isotopes tracers, combined with hydrological modelling approaches can be used to quantify the lake water balance (Krabbenhoft et al. 1990; Gibson and Edwards 2002; Sacks et al. 2014; Bouchez et al. 2016; Arnoux et al. 2017).

In the Middle-Atlas Mountains, considered as the “Moroccan water tower” (Bentayeb and Leclerc 1977), the upper part of the Oum-Er-Rbia” (OER) basin is the major water resource for the downstream irrigated dry plains and is essential to their economic development (Chehbouni et al. 2008). In this region, several natural lakes have documented significant lake level variations in response to climate (Sayad and Chakiri 2010; Sayad et al. 2011; Etebaai et al. 2012; Abba et al. 2012), although the relation between lake behavior and climate change has never been quantitatively assessed. This paper aims at implementing the hydrological modelling of the Azigza lake, in the Middle Atlas. Previous studies have shown that Lake Azigza has recorded significant historical lake level changes (Gayral and Panouse 1954; Flower et al. 1989; Benkaddour et al. 2008; Vidal et al. 2016; Jouve et al. 2018). It was suggested that water level fluctuations are linked to rainfall variations (Flower and Foster 1992) although no quantification of this relation was established. We present the climatic, hydrologic and isotopic data

collected during a 4-year observation period (2012-2016). Then, in order to calibrate the lake model, the ungauged components of the lake water balance are estimated using a step-by-step approach, the last step relying on an isotope mass balance to quantify groundwater inflows and outflows. In the discussion section, the influence of the lake stratification on the isotope mass balance modelling is first assessed. Secondly, based on a 4-year lake water balance simulation, the role of groundwater processes in modulating the lake response to contrasted climatic conditions is discussed, and finally the lake sensitivity to persistent dry conditions is estimated.

Hydrogeological and climatic settings

Belonging to the Oum-Er-Rbia (OER) catchment, Lake Azigza (32° 58' N, 5° 26' W, 1540 m a.s.l.), is a small natural mountain lake located in the Moroccan Middle Atlas (Fig. 1). The lake has a tectono-karstic origin (Hinaje and Ait Brahim 2002) and is located in a relatively undisturbed and forested region, dominated by Cedar (Cedrus Atlantica) and Oak (Quercus) woodland formed on calcareous red soils (Flower and Foster 1992). The study area is situated in the Tabular Middle Atlas, generally made up of Jurassic limestone and dolomite plateau (Lepoutre and Martin 1967). The Azigza lake catchment belongs to the locally designated "High OER (HOER) basin", delineated upstream to the Hansali Dam (Fig. 1). The HOER basin is known for its important hydrological potential and includes the emblematic Oum-Er-Rbia spring system, with an average discharge of 260 $m^3 s^{-1}$. In the different nearby gauged subcatchments, average specific discharges tend to increase with increasing drainage area, from ≈ 170 mm yr^{-1} to ≈ 470 mm yr^{-1} (Fig. 1; Table 1), evidencing the impact of groundwater circulation in this karstic environment. For comparison, the whole OER catchment (48000 km^2) displays a specific discharge of only 25 mm yr^{-1} (Q = 38 $m^3 s^{-1}$) (Hammani et al. 2005). The climate is of Mediterranean subhumid type, characterized by wet winters and dry summers. Mean annual rainfall approaches 900 mm yr^{-1}, most of which falls between October and April, and snow may persist for one or two months; mean annual air temperature is about 12 °C (Martin 1981).

Data and methods

Lake bathymetry and catchment morphology

A precise lake bathymetry was established using an echo-sounder in April 2013 (Fig. 1). The deepest point of the lake (42 m in April 2013) is located at the center of the southeast part of the lake, characterized by steep slopes compared to the western part. In order to account for possible higher lake levels, elevation data over the emerged part of the lake basin were also collected with a Real-Time Kinematic GPS (RTK GPS). Data were incorporated into a 30 m resolution DEM (earthexplorer.usgs.com) covering the remaining part of the lake watershed. A Geographic Information System (GIS) software (ArcGIS 10.3) was used for DEM quality assessment, data conversion, geo-

referencing, profile extraction, interpretation, visualization and calculation of volume and area corresponding to different lake levels. The lake catchment has a surface of 10.2 10^6 m^2, about twenty times the lake surface, with elevation up to 1794 m a.s.l.. It has no outlet and no permanent creek towards the lake. In April 2013, the lake level was 1546 m a.s.l. the lake area was 0.56 10^6 m^2 and the volume was 7.9 10^6 m^3.

Climate data

A meteorological station was settled in November 2014, located 3.7 m above the ground surface, about 30 m above the current lake level and 700 m away from the lake shoreline. Local climatic parameters were measured hourly from November 2014 to May 2016: precipitation (P), air temperature (T_a), relative humidity (rh), atmospheric pressure (P_a), solar radiation (R_s) and wind speed (U). In addition, to cover the remaining observation period, from October 2012 to September 2016, we used daily precipitation from the Tamchachate station, located about 20 km from the lake, at 1685 m a.s.l. (data from the OER Hydraulic Basin Agency), and reanalyzed data (P, T_a, rh, R_s, and incident longwave radiation, R_l) from the European Centre for Medium Range Weather Forecast (ECMWF) ERA-Interim database (Dee et al. 2011). The good correlations found between locally measured T_a, rh, and R_s and ERA Interim data over the common period (r^2 = 0.97, 0.77 and 0.89 respectively) were used to complete the local dataset. Based on daily precipitation, similar rainfall trends were found between the local station and the Tamchachate station, but the common period was too short to establish a robust statistic. We thus used the total rainfall ratio to complete the local dataset: $P_{Azigza} = 0.79 \times P_{Tamchachate}$.

Lake level and water temperature

In April 2013, a reference level was set, and the water level was manually measured approximately each month during the sampling period (April 2013-November 2014). The initial lake level (October 2012) was estimated from a photographic benchmark, compared to the reference level. This lake level time series was complemented by a CTD DIVER, anchored in the eastern part of the lake, that recorded water pressure, temperature and conductivity at an hourly time step from November 2014 to May 2016.

A strong declining trend was observed during the study period (4 m). Over this interannual trend, the lake level showed seasonal variations, with a slight increase in winter (October to April) and a stronger decrease from May to September (Fig. 2a). Based on daily data, a rapid response of lake level variations to precipitation events (≈1 day) was observed.

Three temperature profiles were established in January 2013, April 2014 and September 2015. The water column was homogeneous in January, with temperature ranging between 7.3 and 7.5 °C. During April and September, the lake was stratified with an epilimnion characterized by an average temperature of

17 °C and 21 °C, respectively, while the hypolimnion remained at an average temperature of 7 °C. These layers were separated by a thermocline between 6 and 9 m below the lake surface. These 3 profiles are consistent with previous data (Gayral and Panouse 1954, Benkaddour et al. 2008).

Isotopic data

A monthly sampling of precipitation, lake water and groundwater (well and springs) was performed between October 2012 and November 2014. In addition, a more extensive field campaign was performed in April 2013, including the collection of deep-water samples. Water samples were analyzed for their oxygen ($\delta^{18}O$) and hydrogen ($\delta^{2}H$) isotopic compositions in the Stable Isotope Laboratory at CEREGE. We used either laser spectrometry (Cavity-Ring-Down Laser Spectrometer, WS-CRDS, Picarro L1102-i) or IRMS analysis instruments. Using IRMS, water samples were equilibrated with CO_2 (10h at 291K) and H_2 (2h at 291K with a platinum catalyst) – for $\delta^{18}O$ and $\delta^{2}H$, respectively – in an automated HDO Thermo-Finnigan equilibrating unit before measurement on a dual inlet Delta Plus mass spectrometer. All the samples were replicated. Calibration of measurements was performed following the IAEA reference sheet (IAEA 2009), using three liquid laboratory standards normalized beforehand against V-SMOW, GISP2 and SLAP2 international standards. The values of the isotopic results are presented in the standard notation δ permil (‰) and referenced to Vienna Standard Mean Ocean Water (V-SMOW). The 1σ measurement precision is 0.05 ‰ for $\delta^{18}O$ and 1 ‰ for $\delta^{2}H$.

The weighted average precipitation composition was -7.15 ‰ and -42.6 ‰ for $\delta^{18}O$ and $\delta^{2}H$ respectively, and falls slightly above the Moroccan Meteoric Water Line (MMWL) established by Ait Brahim et al. (2016) ($^{2}H = 7.7 \times \delta^{18}O + 9.2$, $r^2 = 0.93$, Fig. 3). Temporary springs encountered on the southern shore displayed a very stable composition ($\delta^{18}O = -7.70 \pm 0.13$ ‰ and $\delta^{2}H = -46.1 \pm 0.8$ ‰), while groundwater sampled monthly in the well presented a slight variation, from -7.56 ‰ to -6.33 ‰ for $\delta^{18}O$, and from -46.0 ‰ to -38.8 ‰ for $\delta^{2}H$. Following the Moroccan altitude gradient (Ait Brahim et al. 2016), the average precipitation and springwater compositions would correspond to elevations of 1900 m a.s.l. and 2050 m a.s.l. respectively, slightly higher than the catchment maximum elevation.

The lake water isotopic compositions (δ_L) ranged from -7.56 ‰ to -2.30 ‰ and from -46.3 ‰ to -20.7 ‰ for $\delta^{18}O$ and $\delta^{2}H$ respectively, and plot along a well-defined evaporation line ($\delta^{2}H = 4.8 \times \delta^{18}O - 9.9$; $r^2 = 0.97$, n = 80), which crosses the composition of springwater and local precipitation (Fig. 3). The average value calculated from the three sampling locations was -3.43 ‰ for $\delta^{18}O$ and -26.3 ‰ for $\delta^{2}H$ over the whole studied period.

Time evolution (Fig. 2b) shows smoothed seasonal variations at the L1 sampling location, with a maximum during October and a minimum at the beginning of spring. For the other two sampling sites located on the southern shore of the lake, depleted compositions were recorded during rainfall periods,

especially for L2 ($\delta^{18}O$ = -5.77 ‰ in February 2013, -7.56 ‰ in March 2013 and -4.82 ‰ in January 2014). In the absence of visible surface runoff during the sampling, these depleted compositions are attributed to the influence of subsurface inflows. Based on the smoothed variations recorded at L1, seasonal minima were encountered in March-May 2013 ($\delta^{18}O$ = -3.93 ‰ and $\delta^{2}H$ = -28.0 ‰), and in January-April 2014 ($\delta^{18}O$ = -3.70 ‰ and $\delta^{2}H$ = -27.2 ‰), while the most enriched compositions were found in October. The maximum reached in October 2013 ($\delta^{18}O$ = -3.12 ‰ and $\delta^{2}H$ = -20.7 ‰), is lower than the maximum reached in October 2014 ($\delta^{18}O$ = -2.43 ‰ and $\delta^{2}H$ = -23.9 ‰).

The homogeneity of the lake water body was evaluated from a more extensive sampling performed in April 2013. Based on 8 surface water and 7 bottom water samples, well distributed, the water composition was found to be homogeneous, with an average value ($\delta^{18}O$ = -3.90 ± 0.12 ‰ and $\delta^{2}H$ = -27.9 ± 0.4 ‰) very similar to the L1 sampling location ($\delta^{18}O$ = -3.94 ‰ and $\delta^{2}H$ = -28.2 ‰). No bottom lake water samples are available at the end of the summer season.

Lake water and isotope mass balance model

The dynamic lake water balance equation, associated with quantified area–volume–depth relationships, is expressed as follows:

$$\frac{dV}{dt} = S \times (P - E) + Ri + Gi - Go \qquad (1)$$

where, for a daily time step (dt), dV is the lake volume variation (m^3), S = f(V) is the lake surface (m^2) as a function of lake volume, P is the precipitation on the lake surface (m day^{-1}), E is the evaporation from the lake surface (m day^{-1}), and Gi and Go are the groundwater inflows and outflows respectively (m^3 day^{-1}) and Ri is the diffuse surface runoff (m^3 day^{-1}). The lake level simulation (h, in m a.s.l.) was then derived from the h = f(V) relationship (Fig. 1).

The dynamic isotopic mass balance equation is:

$$\frac{d(V.\delta_L)}{dt} = S \times (P.\delta_P - E.\delta_E) + Ri.\delta_P + Gi.\delta_{Gi} - Go.\delta_L \quad (2)$$

where δ is either the $\delta^{18}O$ or $\delta^{2}H$ isotopic composition of each of the water balance components: δ_L for the lake water, which also accounts for the composition of Go, assuming a homogeneous lake water body, δ_P for precipitation water, which also accounts for the composition of Ri, δ_{Gi} for the composition of Gi, taken as the springwater composition. The composition of the water vapor evaporated from the lake, δ_E, was estimated from the Craig and Gordon equation (Craig and Gordon 1965):

$$\delta_E = \frac{(\delta_L - \varepsilon^*)/\alpha - (rh.\delta_A) - \varepsilon_k}{1 - rh + \varepsilon_k} \qquad (3)$$

$$\varepsilon_k = (1 - \mathrm{rh}).\theta.\mathrm{n}.\mathrm{CD} \qquad (4)$$

where α is the equilibrium fractionation factor calculated at T_w, the surface water temperature (Horita and Wesolowski 1994), ε^* is the equilibrium isotopic separation, related to the fractionation factor by $\varepsilon^* = (\alpha - 1)$, ε_K is the kinetic separation, CD a kinetic constant established experimentally ($28.5\ 10^{-3}$ and $25.1\ 10^{-3}$ for ^{18}O and ^{2}H, Merlivat 1978), n = 0.5 for open water bodies, θ is a transport resistance parameter (Gonfiantini 1986; Gat 1996), rh is the relative humidity normalized to T_w, and δ_A the isotopic composition of the ambient moisture. δ_A was estimated from the assumption of an isotopic equilibrium between precipitation and atmospheric vapor ($\delta_A = \delta_P - \varepsilon^*$). All terms are expressed in the decimal notation. The value of θ is generally lower than 1 for a water body whose strong evaporation flux influences the atmospheric boundary layer (Horita et al. 2008). A value of 0.5 has been determined for the eastern Mediterranean Sea (Gat et al. 1996), and for Lake Chad (Bouchez et al. 2016). Here, the θ value was chosen to match the observed slope of the evaporation line (leading to θ = 0.5).

To calculate an annual lake water balance, a steady state is often assumed. The water and isotope mass balance equations (Eq. 1 and 2) are then simplified to express the evaporation-to-input ratio (E_V/I), which represents the degree of closure of the lake:

$$E_V/I = \frac{\delta_I - \delta_L}{\delta_E - \delta_L} \qquad (5)$$

where I is the total annual water inputs ($I = P_v + Ri + Gi$), E_v and P_v the volumetric terms of evaporation and precipitation, accounting for lake surface variations at the daily time step, δ_I is the isotopic composition of inflows, and δ_L is the average annual lake water isotopic composition. When dealing with strongly seasonal systems, all the annual averages have to be weighted by the corresponding fluxes (Gibson and Edwards 2002). For imbalanced annual lake water budgets ($\Delta V/\Delta t \neq 0$), Eq. (5) becomes:

$$I = \frac{\Delta(V.\delta_L)/\Delta t + E_V(\delta_E - \delta_L) - \delta_L \Delta V/\Delta t}{\delta_I - \delta_L} \quad (6)$$

When available, the estimate of $\Delta(V.\delta_L) / \Delta t$ can be based on seasonal variations of V and δ_L, at a given (i) time step, as follows:

$$\frac{\Delta(V.\delta_L)}{\Delta t} = \Sigma(V_{(i)}.\delta_{L(i)} - V_{(i-1)}.\delta_{L(i-1)}) \qquad (7)$$

All calculations were coded in the PYTHON language.

Evaporation estimate

The Penman combination method (Penman 1948) can be applied with synoptic climate data to estimate open-water evaporation (Brutsaert 1982; Jensen et al. 1990; Shuttleworth 1992). It combines the energy balance with an aerodynamic formulation as follows:

$$\lambda_E = (R_n - \Delta S)\frac{D}{D+\gamma} + E_a \frac{\lambda\gamma}{D+\gamma} \quad (8)$$

$$\text{with} \quad E_a = 0.26\,(1 + 0.54\,U_2)\,(e_{SW} - e_a) \quad (9)$$

where R_n is the net input of energy at the lake surface (W m^{-2}), ΔS is the change of energy storage in the water body (W m^{-2}), D is the slope of the saturation vapor pressure curve (Pa K^{-1}) at T_a, γ the psychrometric constant (Pa K^{-1}), U_2 is the wind speed at 2 m above the ground surface (m s^{-1}), e_a the actual vapor pressure of the atmosphere (Pa), e_{sw} the saturated vapor pressure (Pa) at T_w. The first term in the Penman approach relies on available energy, and for lake evaporation estimates, involves accounting for the difference between R_n and ΔS. This has no impact on the total annual rate but it introduces a shift in the seasonal evaporation variation (Giadrossich et al. 2015). The net radiation R_n is the sum of the short wave and long wave energy balances:

$$R_n = R_S\,(1 - a) + R_{nli}\,(1 - a') - R_{nle} \quad (10)$$

where R_s is the incoming (shortwave) solar radiation (W m^{-2}), R_{nli} and R_{nle} the longwave incoming and emitted radiation respectively (W m^{-2}), a is the albedo or shortwave reflectance, and a' the longwave reflectivity. According to the work of Cogley (1979) that computes the albedo as a function of the latitude, a value of 0.08 was taken for a, while a' is assumed to have a constant value equal to 0.03 (Parker et al. 1970). The emitted longwave radiation (R_{nle} in W m^{-2}) is based on the Stefan-Boltzmann law:

$$R_{nle} = \varepsilon_W \times \sigma \times T_W{}^4 \quad (11)$$

where ε_w is the emissivity of water, Anderson (1954) gives this value as 0.97, and σ is the Stefan-Boltzman constant, 5.6697*10^{-8} W m^{-2} K^{-4}. The change in the energy storage term over a given time step Δt is:

$$\Delta S = Z \times C_W \times \rho_W \times \frac{\Delta T_W}{\Delta t} \quad (12)$$

where C_w is the specific heat capacity of water (J kg^{-1} K^{-1}), ρ_w the water density (kg m^{-3}), and Z the layer thickness (m) affected by the temperature variation.

Results

Evaporation rate

Daily lake evaporation was computed between 17 November 2014 and 15 July 2016, using the locally measured climatic parameters (Fig. 4a), completed by the incident longwave radiation, R_{nli} obtained from the ECMWF. Considering the thermal stratification and the constant temperature in the lower layer, ΔS was calculated for the upper layer (Z = 8 m), and smoothed using a 30-day moving average to avoid the instabilities due to the daily time step calculation. The period of energy accumulation ($\Delta S > 0$) spans between February and July, with a maximum (≈ 115 W m^{-2}) at the beginning of May, while the stored energy is released between August and January, with a minimum (≈ - 90 W m^{-2}) at the beginning of November (Fig. 4b). This seasonal behavior is comparable in magnitude to that reported for lakes located under a similar climatic regime: Vegoritis Lake in Greece (510 m a.s.l. and mean depth of 20 m; Gianniou and Antonopoulos 2007), and Baratz Lake in Italy (27 m a.s.l. and mean depth of 5 m; Giadrossich et al. 2015). The computed annual evaporation rate (Fig. 4b) gave an annual value of 1217 mm over the complete 2015 annual cycle.

Annual water balance framework over the 2012-2016 period

The lake volume and surface were computed daily using the bathymetric relations, in order to calculate the water balance of the four annual cycles monitored (October-September periods), and to quantify the sum of ungauged fluxes: Ri+Gi-Go (Eq. 1; Table 2). The evaporation rate was extrapolated over the whole studied period based on the daily ERA Interim climate data, with the correlation found with local data, an average wind speed value, and using an annual ΔS time series approximated by a sinusoidal function, with a 70 W m^{-2} amplitude (Fig. 4b). Precipitation data were based on local measurements for the November 2014 – May 2016 period, and on the Tamchachate station for the rest of the period. ΔV was slightly positive during the first annual cycle, and then remained strongly negative (Table 2). Over the 4-year period studied, the lake level progressively decreased from 1545.7 m a.s.l. in October 2012 to 1542 m a.s.l. in October 2016, which corresponds to a 23 % loss of lake volume.

Calibration of net groundwater flow and diffuse surface runoff using daily lake level

The net groundwater flow (NG = Gi - Go), and Ri were calibrated using the daily lake level record (2014-2016). Considering the rapid reaction of the lake to rainfall (Fig. 2b), and the small size of the catchment, we assume that during dry periods, the lake level variations are only driven by evaporation and groundwater exchanges. Assuming P = Ri = 0, it comes:

$$\mathrm{NG} = \frac{dV}{dt} - \mathrm{S(V)} \times \mathrm{E} \qquad (13)$$

The following criteria were used to select appropriate dry periods: a beginning two days after the last rainfall event, a total duration of at least 4 days with a total precipitation lower than 0.2 mm, and a robust linear trend ($r^2 > 0.8$ for the linear regression applied to $\Delta V/\Delta t$). The latter criterion enables measurement artefacts, or lake level instabilities for which the interpretation is unclear, to be ruled out. A total of 10 periods were isolated, for which an average NG was determined. The resulting time series, referred to as $NG_{ref(1)}$, showed a mainly negative balance, with a minimum in November 2014, and a maximum slightly positive in April 2015 (Fig. 5b).

The subsequent step was to run the lake level simulation, with a linearly interpolated daily NG time series, and to introduce a runoff coefficient (k):

$$Ri = k \times A \times P \qquad (14)$$

with A the lake catchment area. An average runoff coefficient (k = 0.06) was obtained by adjusting simulated and measured lake level. A water balance closure criteria was used: starting with the measured lake level, the simulation fitted the level measured at the end of the calibration period. Given the respective sizes of the catchment (10.2 km^2) and the lake surface (0.5 km^2 on average), the resulting Ri is of the same order of magnitude as the direct precipitation on the lake surface (Table 2).

Extrapolation of NG over 2012-2016

To estimate NG over the whole studied period, Eq. (1) was applied for each interval between two manual lake level data, using the previously calibrated runoff coefficient (k). This led to a complementary time series referred to as $NG_{ref(2)}$, which, combined with $NG_{ref(1)}$, covered the whole 2012-2016 period. Significant seasonal variations were evidenced (Fig. 5b). The maximum was reached between April 19th and June 1st 2013 (5200 m^3 day^{-1}), and the minimum occurred in November 2014 (-7000 m^3 day^{-1}, 4-day average), and in November 2013 (-5600 m^3 day^{-1}, 31-day average).

Then, in order to produce a monthly time series, which is more convenient for rainfall-discharge analysis, a monthly adjustment of NG was performed, based on the lake level simulation, and respecting the quantitative framework given by the combination of $NG_{ref(1)}$ and $NG_{ref(2)}$. The resulting NG time series (Fig. 5b), can be considered as the best evaluation, given the available data. Its seasonal behavior is smoothed and delayed compared to monthly rainfall, with seasonal maxima during spring, that only became positive in 2013 and 2015. Interestingly, NG was almost null between May and September 2016.

At the annual time step, NG values were always negative (Table 2), even when the lake water balance was slightly positive (cycle 1), evidencing the dominance of groundwater seepage. The maximum annual NG was found during the first and the fourth annual cycles (-0.45.10^6 m^3 yr^{-1}), and the minimum

values during the second and the third annual cycles (-0.62 and -0.60 10^6 m^3 yr^{-1}, respectively). This trend does not follow the annual variations in precipitation, since the maximum and minimum precipitation occurred during the first and the fourth cycles respectively.

Groundwater flows partitioning and lake water residence time

The partitioning of NG between Gi and Go is based on the isotope mass balance applied at the annual time step for the two first annual cycles, using daily data (Eq. 6 and 7). Results show the importance of groundwater fluxes, which dominated all other components of the lake water balance (Table 2). Gi was higher than P+Ri, with a strong difference between these two years. Considering the lake catchment area, the Gi values correspond to 261 and 71 mm yr^{-1}, respectively. The Go values were also very different between the two years, and correspond to averages of 8500 and 3700 m^3 day^{-1}, respectively, which is of the same magnitude as the minimum NG reached in November 2013 and 2014 (5600 and 7000 m^3 day^{-1}). These pronounced differences between the two years can be attributed to the decrease in annual precipitation, but the decrease in Gi (-73 %) was stronger than for Go (-56 %), and for P (-48 %). For the 2012-2013 hydrological cycle, which is almost at equilibrium, an average residence time of 2.1 year can be estimated.

Discussion

Impact of the lake stratification on the isotope mass balance

The isotopic homogeneity of the lake water body was assessed in April 2013, but not during fall. Nevertheless, our results suggest that the thermal stratification of the lake water column lead to a progressive isotopic stratification during summer, with a more enriched isotopic composition in the surface layer due to the effect of evaporation. This explains the inability of the model to simulate the observed lake isotopic seasonality, with smaller seasonal amplitudes and delayed maxima compared to the measured values (Fig. 5c, simulation #1), while a lower initial isotopic composition would lead to a better simulation of observed isotopic data (Fig. 5c, simulation #2). To illustrate the effect of lake stratification, simple mass balance calculation allowed us to evaluate the magnitude of the observed seasonal enrichment (+0.85‰ between June 1st and September 7th 2013, and +1.26 ‰ between April 14th and September 7th 2014). Assuming the whole water body is affected, and neglecting groundwater fluxes, the evaporation rates able to explain observed isotopic variations were much higher than the actual lake evaporation (+48 % and +67 %, for 2013 and 2014, respectively). Integrating the water column stratification into the simulation would require much more detailed isotopic data, to characterize the seasonal lake isotopic behavior of the water column, and the depth of sub-aquatic sources (Gi) and sinks (Go), which are probably diverse and localized in such a complex karstic environment.

The impact of the lake stratification on the annual isotope mass balance needs to be assessed, since it leads to overestimating the annual average δ_L compared to that of a homogeneous water body. Considering that the thermocline (≈ 8 m depth) divides the lake water body into two approximately equivalent volumes, the amplitude of the seasonal isotopic enrichment is twice that of the conceptual "equivalent homogeneous lake volume". In addition, the discrepancy between surface and bottom compositions due to the lake stratification is limited to half a year. These simple considerations allowed us to simulate the theoretical impact of the lake stratification on the seasonal behavior of δ_L. The overestimation of annual average δ_L based on surface measurements, compared to the corresponding δ_L of an "equivalent homogeneous lake volume", represents approximately only 15 % of the amplitude of observed seasonal enrichment, i.e. 0.13 ‰ and 0.19‰ for $\delta^{18}O$ during cycle #1 and #2, respectively. This sensitivity analysis showed that despite the amplification of the seasonal lake water isotopic enrichment, the water column stratification only slightly affects the annual mass balance by underestimating groundwater inflows by less than 10 %.

Impact of non-steady state on the isotope mass balance

The steady state isotopic mass balance, expressed as the Ev/I ratio (Eq. 5), has been widely used for quantifying an annual lake water balance (e.g. Gibson and Edwards 2002; Yi et al. 2008; Gibson and Reid 2014; Gibson et al. 2017; Cui et al. 2018). This approach, designed for steady state situations, may lead to wrong estimates in the case of interannual trends. We took the opportunity of our seasonal isotopic sampling to evaluate the error associated with the application of the steady state isotope mass balance to non-steady state situation. During the year 2013-2014 (cycle #2), the lake volume decreased by around 10 %. The steady state application of the isotope mass balance (Eq. 5) gives $E_v/I = 0.29$ (using both $\delta^{18}O$ and $\delta^{2}H$), compared to the reference ratio: $E_v/I = 0.52$ and 0.51 (using $\delta^{18}O$ and $\delta^{2}H$ mass balances, respectively), and would lead to overestimating Gi by 140 %. This comparison points to the importance of a seasonal survey for lake water balance studies.

Magnitude and variations of groundwater exchanges

The shape of monthly NG variations seems to roughly respond to precipitation seasonality, with a time lag of several months after the rainy winter (Fig. 5b). However, annual NG does not follow the precipitation trend, with the driest year (cycle #4) characterized by an annual NG similar to that of the wettest year (cycle #1). Therefore, understanding the relation between rainfall and the groundwater control on the lake water balance requires the partitioning of NG between inflow and outflow.

A major result of the isotopic groundwater partitioning is that groundwater components, both Gi and Go, largely dominate all the other water balance components, even though their difference remains relatively low. Lake Azigza water balance is thus mainly driven by subsurface circulation. In addition,

groundwater fluxes are very different between cycles #1 and #2, for both Gi and Go, while annual precipitations are also strongly contrasted. These Go variations contradicts the previous assumption of a constant seepage rate (Flower and Foster 1992), and suggests that both groundwater fluxes are linked to the amount of precipitation.

Another important result of the isotope water balance is that the magnitude of Gi is consistent with a recharge area equivalent to the lake catchment area, leading to annual values (261 mm and 71 mm) in line with the magnitude of average runoff measured for the smallest gauged catchment in the region (Tamchachate station, 166 mm yr^{-1}, Table 1), and with the corresponding relation between annual precipitation and runoff (Fig. 6). The apparent similarity between the P – Gi relation and the rainfall-runoff relation of the neighboring Tamchachate watershed is consistent with the karstic environment of these upstream catchments, where rivers are typically fed by rapid groundwater circulation. Based on this similarity, the Tamchachate empirical rainfall-runoff relation was used to assess the magnitude of Gi for the two remaining annual cycles. Corresponding Go values were then deduced from annual NG (Table 2) and four estimates of the Azigza annual lake water balance are proposed.

The strongly contrasted climatic situations covered by our studied period provide interesting information on the lake water balance response to precipitation variations. At the annual time scale, a high range of variation was obtained for Gi (1–12 range), while Go also varied along with annual precipitation, but with a lower magnitude (1–5 range). Contrasting with these strong variations, the difference between the two fluxes remained relatively stable (1–1.4 range for NG). The groundwater partitioning suggests that the higher annual NG during 2015-2016 was due to a very low Go and Gi. This is consistent with monthly NG, which became almost null between May and September 2016, suggesting a disconnection of the lake from groundwater circulation. Therefore, except for this particular situation, the concomitant variations of annual Gi and Go together with annual rainfall, indicate that they are probably driven by the same hydraulic gradient.

Lake sensitivity to persistent dry climate conditions

The strong and continuous decreasing trend observed during the studied period raises the question of the future evolution of the lake. Climatic projections suggest an intensification of dry conditions in the Mediterranean area (Tramblay et al. 2013b), and a decrease in rainfall would greatly impact hydrological fluxes. In order to evaluate such impacts, the lake model was used to perform sensitivity analysis.

A first test was performed to simulate the lake level behavior, using the 2015-2016 period as representative of dry conditions: the model was run with the hydroclimatic data of cycle #4, by iterating continuously the same hydrological year. Results led to a complete lake drying after 12 years.

Nevertheless, by maintaining a constant Go, this sensitivity test represents an extreme situation. The lake behavior greatly depends on whether groundwater seepage is permanent or not, and the last part of our study period suggest a disconnection of the lake from groundwater flows. In this karstic environment, groundwater circulation occurs through preferential flowpaths, and groundwater seepage could possibly decrease, or even stop, if the lake level fell below the active water routing structures. A progressive decreasing Go, until the disconnection observed after May 2016, could explain why the seasonal minimum in NG remained relatively high during the end of 2015, compared to the situations of November 2012, 2013 and 2014 (Fig. 5b). This scenario was tested by running the lake model with NG = 0, while keeping the climatic conditions of cycle #4. A lake level decrease of 5.5 m during the same 12-year period was obtained.

Finally, additional sensitivity analysis was performed to evaluate the impact of an increase in evaporation. Its influence remains almost negligible compared to the influence of groundwater flow variations (1-meter difference in 12 years with a 10 % increase of evaporation).

Conclusion

The Azigza lake water balance variations were determined over a 4-year period, which covered contrasted climatic situations and documented strong hydrological differences. A major result is that Lake Azigza water balance is mainly driven by subsurface circulation, with significant interannual variations in groundwater fluxes.

The quantification of groundwater inflow and outflow was achieved by the detailed seasonal water sampling, which allowed us to determine an isotopic mass balance. It was not possible to decipher seasonal variations of groundwater flows because of the influence of the summer thermal stratification, which prevents mixing of the water body. Nevertheless, we showed that the isotopic mass balance is a robust way to partition the groundwater contribution between inflow and outflow, at the annual timescale, given that a sub-annual sampling is available. The short water residence time, estimated at 2 years for 2012-2013, explains the rapid lake level response to climate variations.

The magnitude of groundwater inflow indicates a recharge area consistent with the topographic catchment area, with interannual variations comparable to runoff variations measured in a nearby catchment. Strong variations of groundwater outflow are also evidenced, which contradicts the previous assumption of a constant seepage (Flower and Foster 1992). Moreover, our results suggest that groundwater seepage may be strongly reduced, or even stopped, when the lake level decreases. Monthly NG and groundwater partitioning point to closure of the lake after May 2016, corresponding to threshold level of 1542.5 m a.s.l.. Such a decrease of Go associated to the lake level drop could give the lake a resilience capacity in a context of persistent dry climatic conditions.

Acknowledgements

This work and the associated PhD (RA) were funded by LABEX OT-Med (# ANR-11-LABX-0061) (PHYMOR project) (France), CNRST (Morocco) and PHC Toubkal (Project # 16/38). The support of the LMI-TREMA-Marrakech (IRD) for lake Azigza monitoring is acknowledged. We also particularly thank the SETEL- and SIGEO- CEREGE and IRD-Rabat for logistic support during the field trips (2013 and 2015).

References

Abba H, Nassali H, Benabid M, El Ibaoui H, Chillasse L (2012) Approche physicochimique des eaux du lac dayet Aoua (Maroc). Journal of Applied Biosciences 58:4262–4270

Ait Brahim Y, Bouchaou L, Sifeddine A, Khodri M, Reichert B, Cruz FW (2016) Elucidating the climate and topographic controls on stable isotope composition of meteoric waters in Morocco, using station-based and spatially-interpolated data. Journal of Hydrology 543:305–315. doi: 10.1016/j.jhydrol.2016.10.001

Anderson ER (1954) Energy-budget studies. In: Water-Loss Investigations: Lake Hefner Studies, Technical report. US Geological Survey Professional, Washington, pp 71–119

Arnoux M, Barbecot F, Gibert-Brunet E, Gibson J, Rosa E, Noret A, Monvoisin G (2017) Geochemical and isotopic mass balances of kettle lakes in southern Quebec (Canada) as tools to document variations in groundwater quantity and quality. Environmental Earth Sciences 76:1–14. doi: 10.1007/s12665-017-6410-6

Benkaddour A, Rhoujjati A, Nourelbait M (2008) Hydrologie et sédimentation actuelles au niveau des lacs Iffer et Aguelmam Azigza (Moyen Atlas, Maroc). In: Aouraghe H, Haddoumi H, Hammouti KE (eds) Le quaternaire marocain dans son contexte méditerranéen: actes de la quatrième rencontre des quaternaristes marocains (RQM4). Faculté des Sciences d'Oujda, Oujda, pp 108–118

Bentayeb A, Leclerc C (1977) Le causse moyen atlasique. In: Ressources en Eau du Maroc. Service géologique du Maroc, Rabat, pp 37–84

Bouchez C, Goncalves J, Deschamps P, Vallet-Coulomb C, Hamelin B, Doumnang JC, Sylvestre F (2016) Hydrological, chemical, and isotopic budgets of Lake Chad: A quantitative assessment of evaporation, transpiration and infiltration fluxes. Hydrology and Earth System Sciences 20:1599–1619. doi: 10.5194/hess-20-1599-2016

Brutsaert W (1982) Evaporation into the Atmosphere: Theory, history, and applications. Springer Netherlands, Dordrecht. 299 pp

Chehbouni A, Escadafal R, Duchemin B, Boulet G, Simonneaux V, Dedieu G, Mougenot B, Khabba S, Kharrou H, Maisongrande P, Merlin O, Chaponnière A, Ezzahar J, Er-Raki S, Hoedjes J, Hadria R, Abourida A, Cheggour A, Raibi F, Boudhar A, Benhadj I, Hanich L, Benkaddour A, Guemouria N, Chehbouni AH, Lahrouni A, Olioso A, Jacob F, Williams DG, Sobrino JA (2008) An integrated modelling and remote sensing approach for hydrological study in arid and semi-arid regions: The SUDMED programme. International Journal of Remote Sensing 29:5161–5181. doi: 10.1080/01431160802036417

Cogley JG (1979) The Albedo of Water as a Function of Latitude. Monthly Weather Review 107:775–781. doi: 10.1175/1520-0493(1979)107<0775:TAOWAA>2.0.CO;2

Craig H, Gordon L (1965) Deuterium and oxygen 18 variations in the ocean and the marine atmosphere. In: Tongiogi E (ed) Stable Isotopes in Oceanographic Studies and Paleotemperatures. Pisa: Laboratorio di Geologia Nucleare, Spoleto, Italy, pp 9–130

Cui J, Tian L, Gibson JJ (2018) When to conduct an isotopic survey for lake water balance evaluation in highly seasonal climates. Hydrological Processes 32:379–387. doi: 10.1002/hyp.11420

Dee DP, Uppala SM, Simmons AJ, Berrisford P, Poli P, Kobayashi S, Andrae U, Balmaseda MA, Balsamo G, Bauer P, Bechtold P, Beljaars ACM, van de Berg L, Bidlot J, Bormann N, Delsol C, Dragani R, Fuentes M, Geer AJ, Haimberger L, Healy SB, Hersbach H, Hólm EV, Isaksen L, K\a allberg P, Köhler M, Matricardi M, Mcnally AP, Monge-Sanz BM, Morcrette JJ, Park BK, Peubey C, de Rosnay P, Tavolato C, Thépaut JN, Vitart F (2011) The ERA-Interim reanalysis: Configuration and performance of the data assimilation system. Quarterly Journal of the Royal Meteorological Society 137:553–597. doi: 10.1002/qj.828

Driouech F, Déqué M, Sánchez-Gómez E (2010) Weather regimes-Moroccan precipitation link in a regional climate change simulation. Global and Planetary Change 72:1–10. doi: 10.1016/j.gloplacha.2010.03.004

Etebaai I, Damnati B, Raddad H, Benhardouz H, Benhardouz O, Miche H, et Taieb M (2012) Impacts climatiques et anthropiques sur le fonctionnement hydrogéochimique du Lac Ifrah (Moyen Atlas marocain). Hydrological Sciences Journal 57:547–561. doi: 10.1080/02626667.2012.660158

Filahi S, Tramblay Y, Mouhir L, Diaconescu EP (2017) Projected changes in temperature and precipitation indices in Morocco from high-resolution regional climate models. International Journal of Climatology 37:4846–4863. doi: 10.1002/joc.5127

Flower R, Foster IDL (1992) Climatic implications of recent changes in lake level at Lac Azigza (Morocco). Bulletin de la Société Géologique de France 163:91–96

Flower RJ, Stevenson AC, Dearing JA, Foster IDL, Airey A, Rippey B, Wilson JPF, Appleby PG (1989) Catchment disturbance inferred from paleolimnological studies of three contrasted sub-humid environments in Morocco. Journal of Paleolimnology 1:293–322. doi: 10.1007/BF00184003

Gat JR (1996) Oxygen and Hydrogen Isotopes in the Hydrologic Cycle. Annual Review of Earth and Planetary Sciences 24:225–262. doi: 10.1146/annurev.earth.24.1.225

Gat JR, Shemesh A, Tziperman E, Hecht A, Georgopoulos D, Basturk O (1996) The stable isotope composition of waters of the eastern Mediterranean Sea. Journal of Geophysical Research: Oceans 101:6441–6451. doi: 10.1029/95JC02829

Gayral P, Panouse JB (1954) L'Aguelmame Azigza : Recherches Physiques et Biologiques. Bulletin de la Société des Sciences naturelles et physiques du Maroc 36:135–159

Giadrossich F, Niedda M, Cohen D, Pirastru M (2015) Evaporation in a Mediterranean environment by energy budget and Penman methods, Lake Baratz, Sardinia, Italy. Hydrology and Earth System Sciences 19:2451–2468. doi: 10.5194/hess-19-2451-2015

Gianniou SK, Antonopoulos VZ (2007) Evaporation and energy budget in Lake Vegoritis, Greece. Journal of Hydrology 345:212–223. doi: 10.1016/j.jhydrol.2007.08.007

Gibson JJ, Birks SJ, Jeffries D, Yi Y (2017) Regional trends in evaporation loss and water yield based on stable isotope mass balance of lakes: The Ontario Precambrian Shield surveys. Journal of Hydrology 544:500–510. doi: 10.1016/j.jhydrol.2016.11.016

Gibson JJ, Birks SJ, Yi Y (2016) Stable isotope mass balance of lakes: a contemporary perspective. Quaternary Science Reviews 131:316–328. doi: 10.1016/j.quascirev.2015.04.013

Gibson JJ, Edwards TWD (2002) Regional water balance trends and evaporation-transpiration partitioning from a stable isotope survey of lakes in northern Canada. Global Biogeochemical Cycles 16:1–14. doi: 10.1029/2001GB001839

Gonfinatini R (1986) Environmental isotopes in lake studies. In: Fritz, P. and Fontes JC (ed) Handbook of Environmental Isotope Geochemistry. Elsevier, Amsterdam, pp 113–168

Haghighi AT, Kløve B (2015) A sensitivity analysis of lake water level response to changes in climate and river regimes. Limnologica - Ecology and Management of Inland Waters 51:118–130. doi: 10.1016/j.limno.2015.02.001

Hammani A, Kuper M, Debbarh A, Bouarfa S, Badraoui M, Bellouti A (2005) Evolution de l'exploitation des eaux souterraines dans le périmètre irrigué du Tadla. In: Hammani A, Kuper M, Debbarh A (eds) Actes du Séminaire Modernisation de l'Agriculture Irriguée. IAV Hassan II, Rabat, Maroc, pp 1–8

Hinaje S, Ait Brahim L (2002) Les bassins lacustres du Moyen Atlas, Maroc : un exemple d'activité tectonique polyphasée associée à des structures d'effondrement. In: Comunicações do Instituto Geológico e Mineiro. Hinaje, S., & Ait Brahim, L. (2002). Les bassins lacustres du Moyen Atlas, Maroc : un exemple d'activité tectonique polyphasée associée à des structures d'effondrement. In Comunicações do Instituto Geológico e Mineiro (Vol. 89, pp. 283–294)., Lisboa, pp 283–294

Horita J, Rozanski K, Cohen S (2008) Isotope effects in the evaporation of water: a status report of the Craig – Gordon model. Isotopes in Environmental and Health Studies 44:23–49. doi: 10.1080/10256010801887174

Horita J, Wesolowski DJ (1994) Liquid-vapor fractionation of oxygen and hydrogen isotopes of water from the freezing to the critical temperature. Geochimica et Cosmochimica Acta 58:3425–3437. doi: 10.1016/0016-7037(94)90096-5

IAEA (2009) Reference Sheet for International Measurement Standards. International Atomic Energy Agency Department, Vienna

IPCC (2013) Climate Change 2013: The Physical Science Basis. Contribution of Working Group I to the Fifth Assessment Report of the Intergovernmental Panel on Climate Change. Stocker TF, Qin D, Plattner GK, Tignor M, Allen SK, Boschung J, Nauels A, Xia Y, Bex V, Midgley PM (eds) Cambridge University Press, Cambridge, United Kingdom and New York, NY, USA. 1535 pp

Jensen ME, Burman RD, Allen RG (1990) Evapotranspiration and Irrigation Water Requirements. American Society of Civil Engineers, Manuals and Reports on Engineering Practices no. 70, New York, USA. 360 pp

Jones MD, Cuthbert MO, Leng MJ, McGowan S, Mariethoz G, Arrowsmith C, Sloane HJ, Humphrey KK, Cross I (2016) Comparisons of observed and modelled lake δ18O variability. Quaternary Science Reviews 131:329–340. doi: 10.1016/j.quascirev.2015.09.012

Jouve G, Vidal L, Adallal R, Rhoujjati A, Benkaddour A, Chapron E, Tachikawa K, Bard E, Courp T, Dezileau L, Hebert B, Rapuc W, Simmoneau A, Sonzogni C, Sylvestre F Recent hydrological variability of the Moroccan Middle-Atlas Mountains inferred from micro-scale sedimentological and geochemical analyses of lake sediments. Quaternary Research, accepted 2018

Khomsi K, Mahe G, Tramblay Y, Sinan M, Snoussi M (2016) Regional impacts of global change: Seasonal trends in extreme rainfall, run-off and temperature in two contrasting regions of Morocco. Natural Hazards and Earth System Sciences 16:1079–1090. doi: 10.5194/nhess-16-1079-2016

Krabbenhoft DP, Bowser CJ, Anderson MP, Valley JW (1990) Estimating groundwater exchange with lakes: 1. The stable isotope mass balance method. Water Resources Research 26:2445–2453. doi: 10.1029/WR026i010p02445

Legesse D, Vallet-Coulomb C, Gasse F (2004) Analysis of the hydrological response of a tropical terminal lake, Lake Abiyata (main Ethiopian rift valley) to changes in climate and human activities. Hydrological Processes 18:487–504. doi: 10.1002/hyp.1334

Lepoutre B, Martin J (1967) Le causse moyen atlasique. Les cahiers de la recherche agronomique 24:207–226

Lionello P, Abrantes F, Gacic M, Planton S, Trigo R, Ulbrich U (2014) The climate of the Mediterranean region: research progress and climate change impacts. Regional Environmental Change 14:1679–1684. doi: 10.1007/s10113-014-0666-0

Lyons RP, Kroll CN, Scholz CA (2011) An energy-balance hydrologic model for the Lake Malawi Rift Basin, East Africa. Global and Planetary Change 75:83–97. doi: 10.1016/j.gloplacha.2010.10.010

Martin J (1981) Le Moyen Atlas Central : Etude géomorphologique. Service Géologique du Maroc, Rabat. 482 pp

Merlivat L (1978) Molecular diffusivities of H[sub 2] [sup 16]O, HD[sup 16]O, and H[sub 2] [sup 18]O in gases. The Journal of Chemical Physics 69:2864–2871. doi: 10.1063/1.436884

Parker FL, Krenkel PA, Stevens DB (1970) Physical and engineering aspects of thermal pollution. C R C Critical Reviews in Environmental Control 1:101–192. doi: 10.1080/10643387009381565

Penman HL (1948) Natural Evaporation from Open Water, Bare Soil and Grass. Proceedings of the Royal Society A: Mathematical, Physical and Engineering Sciences 193:120–145. doi: 10.1098/rspa.1948.0037

Rosenberry DO, Lewandowski J, Meinikmann K, Nützmann G (2015) Groundwater - the disregarded component in lake water and nutrient budgets. Part 1: Effects of groundwater on hydrology. Hydrological Processes 29:2895–2921. doi: 10.1002/hyp.10403

Sacks LA, Lee TM, Swancar A (2014) The suitability of a simplified isotope-balance approach to quantify transient groundwater-lake interactions over a decade with climatic extremes. Journal of Hydrology 519:3042–3053. doi: 10.1016/j.jhydrol.2013.12.012

Sayad A, Chakiri S (2010) Impact de l'évolution du climat sur le niveau de Dayet Aoua dans le Moyen Atlas marocain. Sécheresse 21:245–251. doi: 10.1648/sec.2010.0252

Sayad A, Chakiri S, Martin C, Bejjaji Z, Echarfaoui H (2011) Effet des conditions climatiques sur le niveau du lac Sidi Ali (Moyen Atlas, Maroc). Physio-Géo 5:251–268. doi: 10.4000/physio-geo.2145

Shuttleworth W.J. H (1992) Evaporation. In: Maidment DR (ed) Handbook of Hydrology. McGraw-Hill, New York, pp 4.1–4.53

Tramblay Y, El Adlouni S, Servat E (2013a) Trends and variability in extreme precipitation indices over maghreb countries. Natural Hazards and Earth System Sciences 13:3235–3248. doi: 10.5194/nhess-13-3235-2013

Tramblay Y, Ruelland D, Somot S, Bouaicha R, Servat E (2013b) High-resolution Med-CORDEX regional climate model simulations for hydrological impact studies: A first evaluation of the ALADIN-Climate model in Morocco. Hydrology and Earth System Sciences 17:3721–3739. doi: 10.5194/hess-17-3721-2013

Troin M, Vallet-Coulomb C, Sylvestre F, Piovano E (2010) Hydrological modelling of a closed lake (Laguna Mar Chiquita, Argentina) in the context of 20th century climatic changes. Journal of Hydrology 393:233–244. doi: 10.1016/j.jhydrol.2010.08.019

Troin M, Vrac M, Khodri M, Caya D, Vallet-Coulomb C, Piovano E, Sylvestre F (2016) A complete hydro-climate model chain to investigate the influence of sea surface temperature on recent hydroclimatic variability in subtropical South America (Laguna Mar Chiquita, Argentina). Climate Dynamics 46:1783–1798. doi: 10.1007/s00382-015-2676-0

Vallet-Coulomb C, Gasse F, Robison L, Ferry L, Van Campo E, Chalié F (2006) Hydrological modeling of tropical closed Lake Ihotry (SW Madagascar): Sensitivity analysis and implications for paleohydrological reconstructions over the past 4000 years. Journal of Hydrology 331:257–271. doi: 10.1016/j.jhydrol.2006.05.026

Vidal L, Rhoujjati A, Adallal R, Jouve G, Bard E, Benkaddour A, Chapron E, Courp T, Dezileau L, Garcia M, Hebert B, Simmoneau A, Sonzogni C, Sylvestre F, Tachikawa K, Vallet-Coulomb C, Viry E (2016) Past hydrological variability in the Moroccan Middle Atlas inferred from lakes and lacustrine sediments. In: Sabrié M-L, Gibert-Brunet E, Mourier T (eds) The Mediterranean Region under Climate Change, IRD. AllEnvi, pp 57–69

Yi Y, Brock BE, Falcone MD, Wolfe BB, Edwards TWD (2008) A coupled isotope tracer method to characterize input water to lakes. Journal of Hydrology 350:1–13. doi: 10.1016/j.jhydrol.2007.11.008

Figure captions

Fig. 1 a) Location of the Oum Er Rbia (OER) basin in Morocco; b) High OER basin delineated at Hansali dam; c) Azigza Lake bathymetry (modified from Vidal et al. 2016) with the location of water sampling (L1, L2, L3 for lake water, W for well water and S for springs) and meteorological station (red star); d) Relation between lake water level, area, and volume (observed lake level range in grey)

Fig. 2 a) Lake level and precipitation time series between October 2012 and October 2016, with manual measurements (black crosses) and continuous lake level record (red line). Daily precipitation is either measured locally (blue) or derived from Tamchachate station (purple; see text); b) Lake water isotopic composition ($\delta^{18}O$) at the three sampling locations

Fig. 3 $\delta^{18}O$-$\delta^{2}H$ cross plots of well, springs, and lake data, with the corresponding evaporation line (dash-dotted line), weighted average precipitation (red) and the Moroccan Meteoric Water Line (black line, Ait Brahim et al. (2016))

Fig. 4 a) Meteorological variables measured at the Azigza station; b) Daily evaporation (blue), with corresponding ΔS (red) and its sinusoidal approximation (dotted black line)

Fig. 5 a) Simulated (green) and measured (black crosses and red line) lake level, with daily precipitation (same as Fig. 2) and dry periods used for $NG_{ref(1)}$ calibration (grey shadow); b) $NG_{ref(1)}$ (black), $NG_{ref(2)}$ (purple) and simulated NG time series (blue-red histogram) and monthly precipitation; c) Simulation of lake water $\delta^{18}O$, with monthly values of Gi calculated from the adjusted NG (Gi= NG+Go) using two initial isotopic composition (#1 green line and #2 blue line)

Fig. 6 Relation between annual rainfall and runoff at the Tamchachate catchment, compared to Azigza P and Gi values for 2012-2013 and 2013-2014

Figure

Click here to access/download;Figure;Figure 1 Adallal et al REEC.jpg

Fig. 1

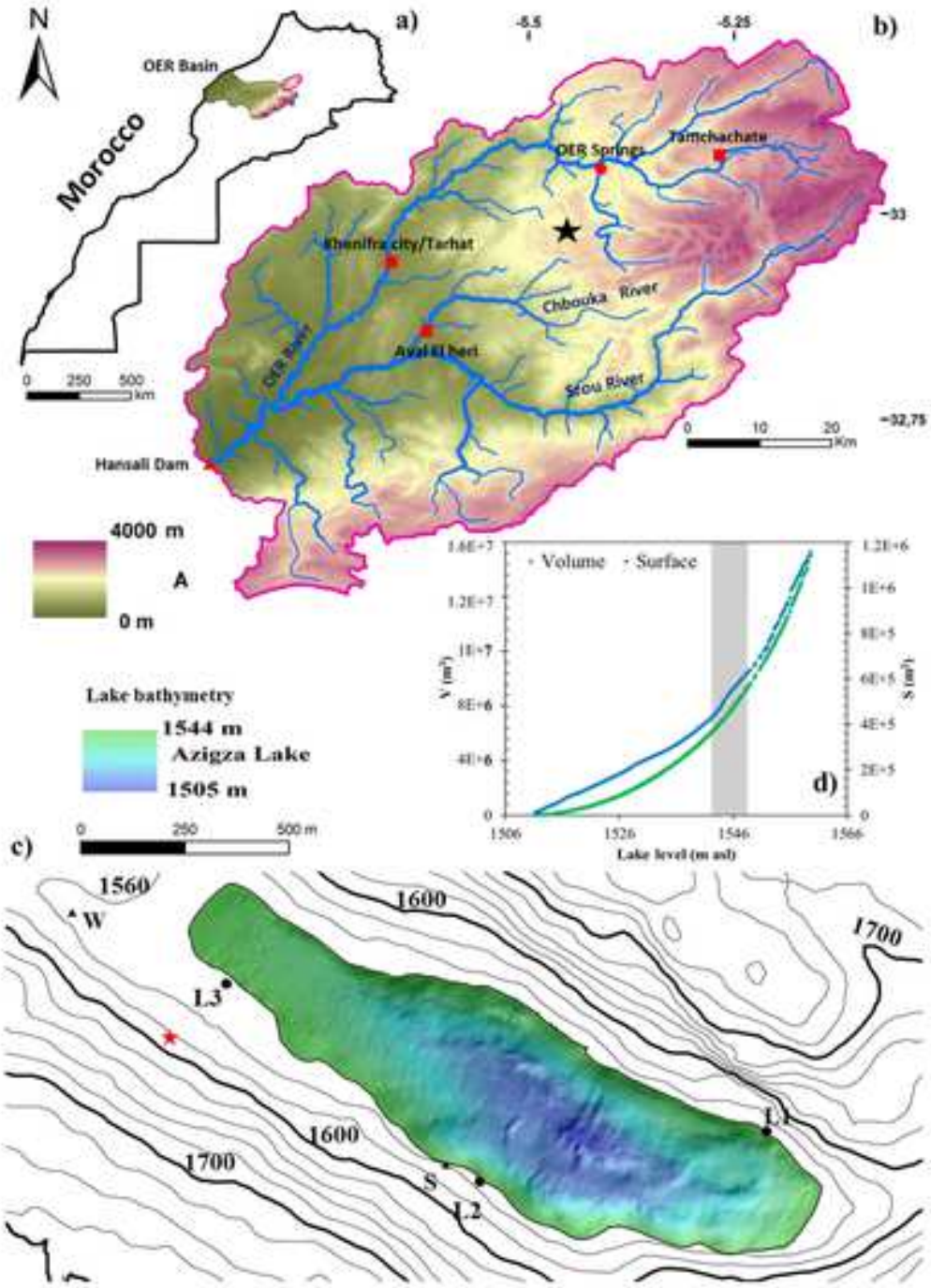

Figure

Click here to access/download;Figure;Figure 2 Adallal et al REEC.jpg

Fig. 2

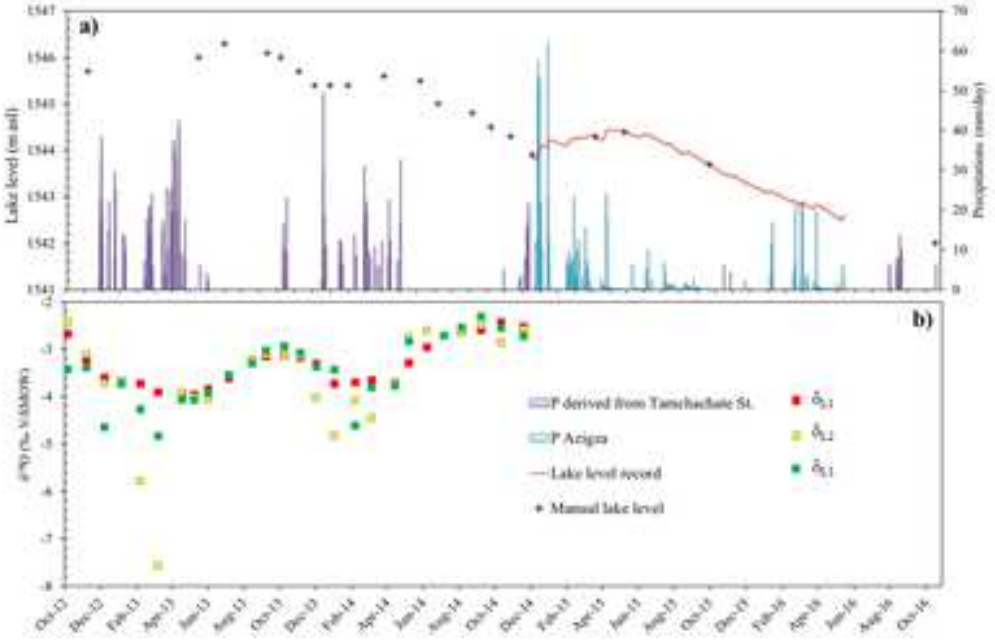

Figure

Click here to access/download;Figure;Figure 3 Adallal et al REEC.jpg

Fig. 3

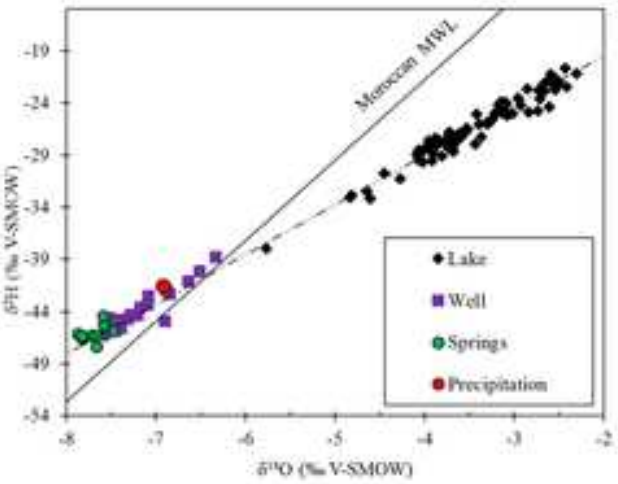

Figure

Click here to access/download;Figure;Figure 4 Adallal et al REEC.jpg

Fig. 4

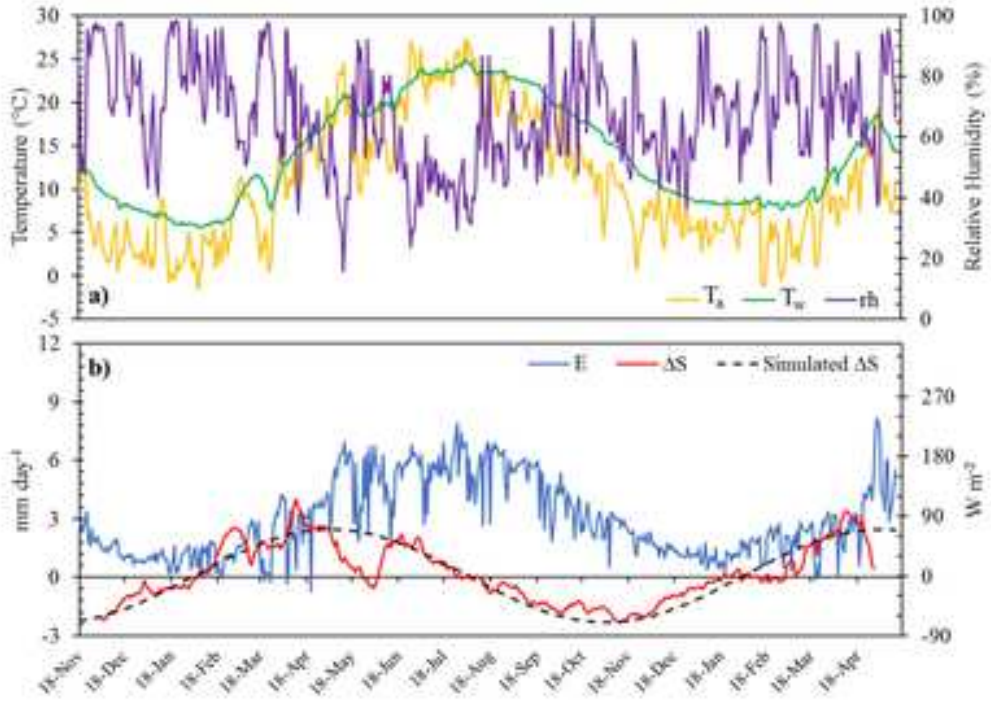

Figure

Click here to access/download;Figure;Figure 5 Adallal et al REEC.jpg

Fig. 5

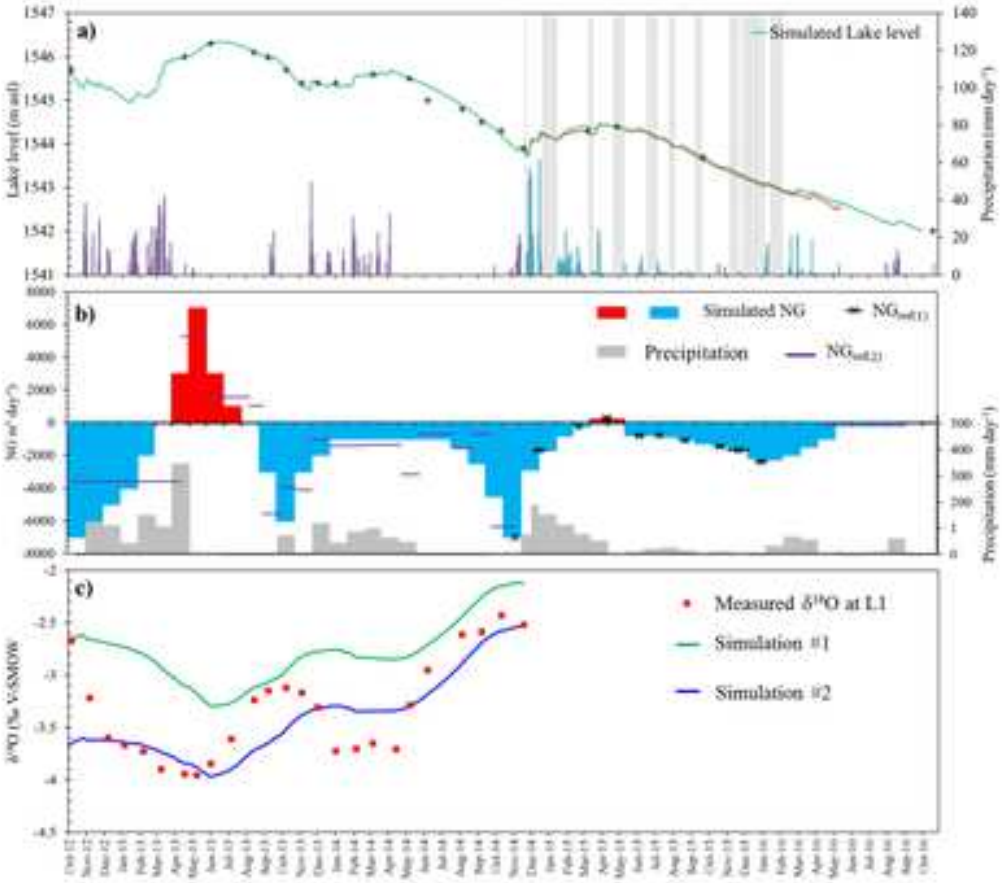

Figure

Click here to access/download;Figure;Figure 6 Adallal et al REEC.jpg

Fig. 6

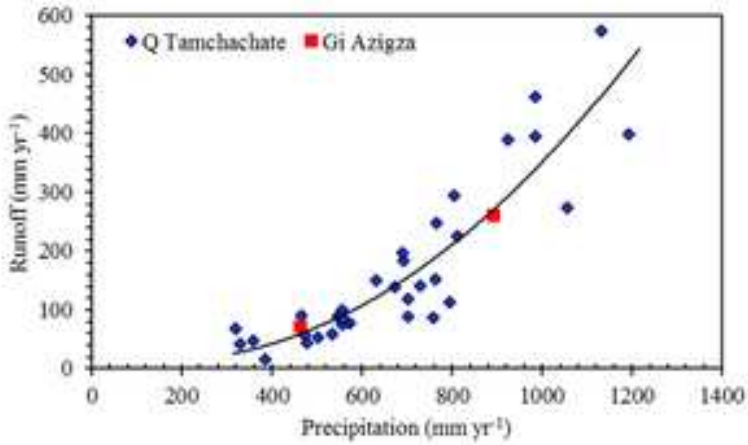

Table

Station	altitude (m a.s.l.)	drainage area (km^2)	specific discharge ($mm\ yr^{-1}$)	Q mean ($m^3\ s^{-1}$)	recording period
Tamchachate	1685	132	166	0.7	1975-2011
			(173)	(0.72)	(1975-1990)
Aval El heri	830	308	245	2.4	1975-2011
			(254)	(2.48)	(1975-1990)
Tarhat	873	1113	468	16.5	1975-1990

Table 1 Hydrological characteristics of three sub-basins belonging to the HOER basin

Table

	P	E	ΔV	Ri + Gi – Go	Ri	NG	Gi	Go	E_v/I
Cycle 1 2012-2013	0.54 10^6 (892 mm)	0.66 10^6	+0.04 10^6	0.16 10^6	0.60 10^6	-0.45 10^6	2.65 10^6 (261 mm)	3.10 10^6	0.17
Cycle 2 2013-2014	0.26 10^6 (462 mm)	0.65 10^6	-0.73 10^6	-0.33 10^6	0.29 10^6	-0.62 10^6	0.71 10^6 (71 mm)	1.34 10^6	0.52
Cycle 3 2014-2015	0.37 10^6 (781 mm)	0.59 10^6	-0.36 10^6	-0.14 10^6	0.46 10^6	-0.60 10^6	2.11 10^6 (199 mm)	2.71 10^6	
Cycle 4 2015-2016	0.12 10^6 (272 mm)	0.54 10^6	-0.71 10^6	-0.29 10^6	0.17 10^6	-0.45 10^6	0.21 10^6 (20 mm)	0.66 10^6	

Table 2 Annual water balance components (m^3 yr^{-1}) resulting from the step-by-step calibration procedure (see text for details)